

# Effect of micro-nano-hybrid structured hydroxyapatite bioceramics on osteogenic and cementogenic differentiation of human periodontal ligament stem cell via Wnt signaling pathway

Lixia Mao,<sup>1,\*</sup> Jiaqiang Liu,<sup>1,\*</sup>  
Jinglei Zhao,<sup>1</sup> Jiang Chang,<sup>2</sup>  
Lunguo Xia,<sup>1</sup> Lingyong  
Jiang,<sup>1</sup> Xiuhui Wang,<sup>2</sup>  
Kaili Lin,<sup>2,3</sup> Bing Fang<sup>1</sup>

<sup>1</sup>Center of Craniofacial Orthodontics, Department of Oral and Cranio-maxillofacial Science, Top Priority Clinical Medical Center of Shanghai Municipal Commission of Health and Family Planning, Ninth People's Hospital Affiliated to Shanghai Jiao Tong University, School of Medicine, Shanghai Jiao Tong University, <sup>2</sup>State Key Laboratory of High Performance Ceramics and Superfine Microstructure, Shanghai Institute of Ceramics, Chinese Academy of Sciences, <sup>3</sup>Shanghai Engineering Research Center of Tooth Restoration and Regeneration, School of Stomatology, Tongji University, Shanghai, People's Republic of China

\*These authors contributed equally to this work

Correspondence: Kaili Lin  
Shanghai Engineering Research Center  
of Tooth Restoration and Regeneration,  
School of Stomatology, Tongji University,  
399 Middle Yanchang Road, Shanghai 200072,  
People's Republic of China  
Email lklecnu@aliyun.com

Bing Fang  
Center of Craniofacial Orthodontics,  
Department of Oral and Cranio-maxillofacial  
Science, Top Priority Clinical Medical Center  
of Shanghai Municipal Commission of Health  
and Family Planning, Ninth People's Hospital  
Affiliated to Shanghai Jiao Tong University,  
School of Medicine, Shanghai Jiao Tong  
University, 639 Zhizaoju Road, Shanghai  
200011, People's Republic of China  
Email fangbing@sjtu.edu.cn

**Abstract:** The surface structure of bioceramic scaffolds is crucial for its bioactivity and osteoinductive ability, and in recent years, human periodontal ligament stem cells have been certified to possess high osteogenic and cementogenic differential ability. In the present study, hydroxyapatite (HA) bioceramics with micro-nano-hybrid surface (mnHA [the hybrid of nanorods and microrods]) were fabricated via hydrothermal reaction of the  $\alpha$ -tricalcium phosphate granules as precursors in aqueous solution, and the effects of mnHA on the attachment, proliferation, osteogenic and cementogenic differentiations of human periodontal ligament stem cells as well as the related mechanisms were systematically investigated. The results showed that mnHA bioceramics could promote cell adhesion, proliferation, alkaline phosphatase (ALP) activity, and expression of osteogenic/cementogenic-related markers including runt-related transcription factor 2 (Runx2), ALP, osteocalcin (OCN), cementum attachment protein (CAP), and cementum protein (CEMP) as compared to the HA bioceramics with flat and dense surface. Moreover, mnHA bioceramics stimulated gene expression of low-density lipoprotein receptor-related protein 5 (*LRP5*) and  $\beta$ -catenin, which are the key genes of canonical Wnt signaling. Moreover, the stimulatory effect on ALP activity and osteogenic and cementogenic gene expression, including that of ALP, OCN, CAP, CEMP, and Runx2 of mnHA bioceramics could be repressed by canonical Wnt signaling inhibitor dickkopf1 (*Dkk1*). The results suggested that the HA bioceramics with mnHA could act as promising grafts for periodontal tissue regeneration.

**Keywords:** surface topography, periodontal ligament stem cells, Wnt signaling pathway, bioceramics, periodontal reconstruction

## Introduction

Clinically, accidental trauma or periodontal diseases may result in destruction of the periodontal structure, which includes hard tissues (alveolar bone and root cementum) and soft tissue (periodontal ligament). Besides, the high prevalence of alveolar fenestrations and dehiscences were found in skull studies.<sup>1,2</sup> Loss of periodontal support tissue will lead to loosening of the teeth and affect oral function, while conventional periodontal surgical approaches such as root surface conditioning or guided tissue regeneration result in limited new bone, cementum, and periodontal ligament formation. Moreover, the formation of new bone and cementum with supportive periodontal ligament is the ultimate objective for periodontal tissue regeneration, but current regeneration therapies are incapable of achieving this in a predictable way.<sup>3,4</sup>

Periodontal ligament derived stem cells (PDLSCs) have been shown to possess multidifferentiation potential and exhibit an immune phenotype similar to bone marrow derived mesenchymal stem cells (BMSCs). More importantly, in addition to the ability to differentiate into osteoblast-like cells and adipocytes, PDLSCs can also specifically differentiate into periodontal cells, such as cementoblast-like cells and collagen forming cells *in vitro*, and they possess the capacity to generate a cementum/PDL-like structure when they were transplanted into nude mouse and preclinical periodontal defect models.<sup>5–12</sup> Conventional hydroxyapatite ( $\text{Ca}_{10}(\text{PO}_4)_6(\text{OH})_2$ , HA) bioceramics had been used in periodontal bone tissue repair for their chemical similarity to bone mineral and their excellent biological activity and osteoconductivity.<sup>13</sup> However, it is reported that HA bioceramics lack osteoinductive ability, and consequently possess limited ability to form an interface with new bone tissue and hence hamper the new bone formation. Moreover, there was no study reporting that HA bioceramics possess the ability to stimulate osteogenic/cementogenic differentiation of PDLSCs.<sup>14</sup>

Most studies showed that the surface topography on biomaterial scaffolds played an important role in regulating cell behaviors such as adhesion, proliferation, differentiation, cytoskeletal organization, apoptosis, and gene expression.<sup>15–17</sup> More importantly, our previous studies have reported that HA bioceramics with nanosheet, nanorod, and micro-nano-hybrid (the hybrid of nanorod and microrod) surfaces could be fabricated by hydrothermal reaction of the  $\alpha$ -tricalcium phosphate ( $\alpha$ - $\text{Ca}_3(\text{PO}_4)_2$ ,  $\alpha$ -TCP) precursors in different aqueous solutions. *In vitro* studies showed that the nano-structured HA bioceramics could stimulate cell adhesion, proliferation, and osteogenic differentiation of BMSCs and adipose-derived stem cells (ASCs), while the mnHA achieved the best stimulatory effect.<sup>18–20</sup> However, whether the HA bioceramics with mnHA could have an enhanced effect on osteogenic and cementogenic differentiation of PDLSCs is largely unknown.

Wnt signaling pathway is a complex protein network that regulates different processes related to cell growth, differentiation, function, and apoptosis during embryonic development, tumorigenesis, and normal physiological process of adults. Recent studies have reported that canonical Wnt signaling pathway plays an important role in skeletal development and homeostasis.<sup>21,22</sup> It has been demonstrated that canonical Wnt signaling modulates most aspects of osteoblast physiology including proliferation, differentiation, bone matrix formation, and apoptosis as well as

osteoclast physiology and bone resorption.<sup>23</sup> Furthermore, activation of the canonical Wnt signaling cannot only lead to the differentiation of periodontal ligament cells (PDLs) into osteogenic lineage along with the stimulation of osteogenic gene, but also induce cementogenic differentiation of PDLs *in vitro* and *in vivo*.<sup>24,25</sup> Moreover, recent studies reported that the ionic products and surface topography of bioactive materials could promote osteoblast differentiation of human MSCs via activation of canonical Wnt signaling pathway.<sup>14,26–28</sup> But whether the canonical Wnt signaling pathway is responsible for the osteogenic and cementogenic effect of mnHAs on human periodontal ligament derived stem cells (hPDLSCs) has not been reported previously and needs to be verified.

In this study, it is hypothesized that the HA bioceramics with mnHA may induce osteogenic and cementogenic differentiation of hPDLSCs via activation of canonical Wnt signaling pathway. Therefore, HA bioceramics with mnHA were fabricated via hydrothermal transformation method using  $\alpha$ -TCP ceramics as precursors, and the effects of mnHA on attachment, proliferation, and osteogenic differentiation of hPDLSCs as well as the related mechanisms were systematically investigated. Furthermore, the key genes of canonical Wnt signaling pathway and the effect of Wnt signaling pathway inhibitor dickkopf1 (Dkk1) on hPDLSCs seeded on mnHA were explored *in vitro*.

## Materials and methods

### Preparation and characterization of the mnHA

In the present study, the HA bioceramics with mnHA (the hybrid of nanorods and microrods) were fabricated via hydrothermal transformation method as described in our previous studies.<sup>19,29</sup> Briefly, the  $\alpha$ -TCP ceramics with diameter of 10 mm and height of 3 mm were dry-pressed using  $\alpha$ -TCP powders and then sintered at 1,350°C for 5 hours. The obtained  $\alpha$ -TCP ceramics were used as the precursors. Then the mnHAs of HA bioceramics were obtained through hydrothermal treatment of the  $\alpha$ -TCP ceramic precursors in aqueous water at 180°C for 24 hours. After hydrothermal reaction, the obtained samples, labeled as mnHA, were washed in deionized water several times. HA bioceramics with traditional flat and dense surface were fabricated by dry-pressing the HA powders into pellets with diameter of 10 mm and height of 3 mm. Then the pellets were sintered at 1,100°C for 3 hours, and the obtained ceramic samples were used as control group. The surface morphology of the samples of the HA bioceramics was

observed by scanning electron microscopy (SEM; JEOL, Tokyo, Japan).

## The isolation, cultivation, and identification of hPDLSCs

PDLCS were obtained from healthy premolars that had been extracted due to orthodontic demands. Written informed consent was obtained from all the patients, and the study was approved by the Ethics Committee of Ninth People's Hospital Affiliated to Shanghai Jiao Tong University. Briefly, the periodontal ligament tissues, which were scraped from the middle third of the root surfaces, were minced into 1 mm cubes before being placed in 100 mm-diameter culture dishes. The tissues were incubated in alpha-minimum essential medium ( $\alpha$ -MEM; Hyclone, Logan, UT, USA) supplemented with 10% fetal bovine serum (FBS; Gibco, Waltham, MA, USA) and 1% penicillin–streptomycin (Gibco) at 37°C in a humidified atmosphere of 5% CO<sub>2</sub> and 95% humidity. To obtain STRO-1<sup>+</sup> PDLSCs, human PDLCS were indirectly sorted using immune-magnetic beads (Miltenyi Biotec, Cologne, Germany) according to the manufacturer's protocol as previously described.<sup>30,31</sup> Approximately 6% of PDLCS can be harvested by STRO-1-mediated magnetic-activated cell sorting method, and these were named PDLSCs.

Chamber slide cultures of hPDLSCs at passage 4 were fixed with 4% paraformaldehyde for 30 minutes and then washed with phosphate-buffered saline (PBS) three times. Then the cultures were treated with PBS/0.1% Triton X-100 to permeabilize the cell membrane for 15 minutes followed by blocking with 1% bovine serum albumin for 20 minutes and were then incubated with primary antibody (mouse anti-human S100, CK, Vimentin, STRO-1; Santa Cruz Biotechnology, Santa Cruz, CA, USA) in blocking solution overnight at 4°C. After being washed, the secondary goat anti-mouse antibodies (Santa Cruz Biotechnology) were added in blocking solution for 2 hours followed by adding phalloidin–tetramethylrhodamine B isothiocyanate (TRITC; Sigma-Aldrich, St Louis, MO, USA) for 45 minutes and 4',6-diamidino-2-phenylindole dihydrochloride (DAPI; Sigma-Aldrich) for 5 minutes in the dark. Finally, the cells were detected by confocal laser scanning microscope (CLSM; Leica, Wetzlar, Germany) to observe the expression of S100, CK, Vimentin, STRO-1. Moreover, to identify the MSC phenotypic characterization of hPDLSCs, 5×10<sup>5</sup> cells at passage 4 were digested to form single-cell suspensions. Conjugated monoclonal antibodies for human CD29, CD44, CD45, CD90, and CD146 (eBioscience, San Diego, CA, USA) labeled with fluorescein isothiocyanate were then

added directly to the suspensions for 45 minutes in the dark. After being washed twice in PBS, the cells were analyzed by FACSCalibur flow cytometer (BD Biosciences, San Jose, CA, USA).

## Adhesion and morphological feature of hPDLSCs cultured on HA bioceramics

The mnHA and HA samples were immersed in  $\alpha$ -MEM overnight after sterilization. Then, the bioceramics were seeded with 1 mL cell suspension containing 2×10<sup>4</sup> cells each well in 24-well plates, and the plates were maintained at 37°C in 5% CO<sub>2</sub> at 95% humidity. After 6 hours, the samples were collected for SEM observation and CLSM observation. As for SEM observation, the samples of cell/ceramic constructs were fixed with 2.5% glutaraldehyde overnight at 4°C. They were then dehydrated in a graded ethanol series and dried in tetramethylsilane. Finally, the samples were sputtered with gold and then were observed by SEM. As for CLSM observation, the samples were fixed, blocked, and permeabilized as described earlier. Then, the cytoskeletons were labeled by TRITC for 45 minutes followed by labeling the nuclei by DAPI for 5 minutes in the dark. Finally, the samples were observed by CLSM.

## MTT assay for cell proliferation

The hPDLSCs of passage 4 were cultured on HA and mnHA samples for 1, 4, and 7 days, respectively. The three pieces of cell/ceramic constructs in each group were assessed for the cell vitality by 3-(4,5-dimethylthiazol-2-yl)-2,5-diphenyltetrazolium bromide (MTT; Sigma-Aldrich) assay as previously reported.<sup>18</sup> Then 400  $\mu$ L  $\alpha$ -MEM supplemented with 40  $\mu$ L of 5 mg/mL MTT solution was added into each well followed by sample incubation at 37°C to allow formazan formation. Four hours later, the solution with MTT was discarded and replaced by 400  $\mu$ L dimethyl sulfoxide (DMSO, Sigma-Aldrich) to dissolve the formazan crystals. The optical density was measured at 490 nm on the Multi-Detection Microplate Reader (Bio-tek, Winooski, VT, USA). In the meantime, an additional standard curve for MTT assay was performed. As previously reported, the cells were seeded in 96-well plates with different densities of 5×10<sup>3</sup>, 1×10<sup>4</sup>, 1.5×10<sup>4</sup>, 2×10<sup>4</sup>, and 2.5×10<sup>4</sup> cell/well and cultured in  $\alpha$ -MEM, and then the cell number was quantified by a cell standard curve.<sup>32</sup> All experiments were conducted in triplicate.

## Alkaline phosphatase activity assay

Alkaline phosphatase (ALP) staining was performed using ALP staining kit (JianCheng Bioengineering, Nanjing,

People's Republic of China) at day 10 after hPDLSCs were seeded on HA and mnHA samples, respectively. Moreover, ALP activity quantitative assay was performed using ALP assay kit (JianCheng) at days 4 and 7 after cell seeding. Briefly, the samples were rinsed with PBS three times to remove the medium. The hPDLSCs in each sample were lysed in 100  $\mu$ L Ripa Lysis Buffer (Beyotime, Nantong, People's Republic of China) and the lysates were centrifuged at 12,000 rpm for 10 minutes at 4°C. The supernatant and reagent were added to a 96-well plate according to the manufacturer's instruction, followed by incubation at 37°C for 15 minutes and was measured at 520 nm using microplate reader. The total protein content was measured by the bicinchoninic acid protein assay kit (Thermo Scientific, Melbourne, VIC, Australia), read at 562 nm and calculated according to a series of albumin standards. Finally, the relative ALP activity was normalized to the total protein content at the end of the experiment. All experiments were conducted in triplicate.

## Quantitative real-time polymerase chain reaction (PCR)

To evaluate the osteogenic and cementogenic gene expression, such as runt-related transcription factor 2 (*Runx2*), ALP, osteocalcin (OCN), cementum attachment protein (CAP), and cementum protein (CEMP) and Wnt signaling pathway-related gene expression, such as low-density lipoprotein receptor-related protein 5 (*LRP5*) and  $\beta$ -catenin, total RNA was isolated from hPDLSCs cultured on HA and mnHA samples at days 1, 4, and 7, respectively. Total

RNA was extracted by Trizol reagent (Invitrogen, Waltham, MA, USA), and then, purified RNA was used to synthesize complementary DNA (cDNA) with the PrimeScript 1st Strand cDNA Synthesis kit (Takara, Tokyo, Japan) according to the manufacturer's instructions. Real-time PCR analysis was performed using the SYBR Green PCR kit (Takara) on the Bio-Rad real-time PCR system (Bio-Rad, Hercules, CA, USA) to evaluate the gene markers, and glyceraldehyde-3-phosphate dehydrogenase (*GAPDH*) was used as a housekeeping gene. The primers are listed in Table 1. All experiments were conducted in triplicate.

## Dkk1 treatment

The hPDLSCs seeded on mnHA samples were cultured in medium supplemented with the soluble Wnt inhibitor human recombinant Dkk1 (100 ng/mL; PeproTech, Rocky Hill, NJ, USA). After being cultured for 7 days, ALP staining was performed as described previously. Total RNA was extracted and synthesized to cDNA, while real-time PCR was performed to analyze the gene expression of  $\beta$ -catenin, *LRP5*, *ALP*, *Runx2*, *CAP*, *CEMP*, and *OCN* according to the methods already mentioned. The cells seeded on mnHA bioceramics without Wnt signaling inhibitor were considered as the control group. All experiments were conducted in triplicate.

## Statistical analysis

The results were presented as mean  $\pm$  standard deviation of at least three replicates for each experiment. All data were

**Table 1** Specific primers used for real-time PCR

Gene	Primer sequence	Length (bp)
<i>Runx2</i>	Reverse: 5'-TCTTAGAACAAATTCTGCCCTTT-3' Forward: 5'-TGCTTTGGTCTTGAAATCACA-3'	136
<i>ALP</i>	Reverse: 5'-TTGACCTCCTCGGAAGACACTC-3' Forward: 5'-CCATACAGGATGGCAGTGAAGG-3'	155
<i>OCN</i>	Reverse: 5'-GGCGCTACCTGTATCAATGGC-3' Forward: 5'-TGCCTGGAGAGGAGCAGAACT-3'	208
<i>CAP</i>	Reverse: 5'-GCGATGTCGTAGAGGTGAGCC-3' Forward: 5'-CTGCGCGCTGCACATGG-3'	165
<i>CEMP</i>	Reverse: 5'-CCCTTAGGAAGTGGCTGTCCAG-3' Forward: 5'-GGGCACATCAAGCACTGACAG-3'	258
<i>LRP5</i>	Reverse: 5'-TGGATAGGGGTCTGAGTCCG-3' Forward: 5'-GTACCCGCCGATCCTGAAC-3'	244
$\beta$ -catenin	Reverse: 5'-CCCTGCTCACGCAAAGGT-3' Forward: 5'-GCTACTGTTGGATTGATTCGAAATC-3'	68
<i>GAPDH</i>	Reverse: 5'-CCTGCACCACCAACTGCTTA-3' Forward: 5'-AGGCCATGCCAGTGAGCTT-3'	246

**Abbreviations:** PCR, polymerase chain reaction; *Runx2*, runt-related transcription factor 2; *ALP*, alkaline phosphatase; *OCN*, osteocalcin; *CAP*, cementum attachment protein; *CEMP*, cementum protein; *LRP5*, lipoprotein receptor-related protein 5; *GAPDH*, glyceraldehyde-3-phosphate dehydrogenase.

analyzed by two-tailed unpaired Student's *t*-test or one way analysis of variance using SPSS 17.0 software (SPSS Inc., Chicago, IL, USA). A value of  $P < 0.05$  was considered to be statistically significant.

## Results

### Characteristics of hPDLSCs

To assess stem-cell-like characteristics of the cells isolated from human periodontal ligament, we identified stem cell markers by immune-cytochemical staining and fluorescence-activated cell sorting (FACS) analysis. As shown in Figure 1A, immunocytochemical staining showed that the hPDLSCs expressed the mesenchymal cell marker Vimentin, neurocyte marker S-100 as well as the stem cell marker STRO-1. In contrast, cytokeratin was absent in hPDLSCs. The FACS analysis showed that the cells expressed markers of MSCs such as CD29, CD44, CD90, and was negative for hematopoietic stem cell marker such as CD45 (Figure 1B). It is also observed that 32.9% hPDLSCs expressed the cell surface antigen CD146, which is present on endothelial and smooth muscle cells.

### Characterization of HA bioceramics with mnHA

The surface morphology of the control HA bioceramic was fully flat and dense, and the average granule size was 0.9  $\mu\text{m}$  (Figure 2A). The HA bioceramics hydrothermally transformed from  $\alpha$ -TCP ceramic precursors fabricated in  $\text{CaCl}_2$  solution exhibited hybrid of nanorods and microrods (Figure 2B). The diameter of the nanorods was approximately 80–120 nm, while the diameter of the microrods was approximately 1–4  $\mu\text{m}$ . The length of the hybrid rods was in the range of 10–20  $\mu\text{m}$ . The X-ray powder diffraction results indicated that the bioceramics could be identified as pure HA phase, and also suggested that the  $\alpha$ -TCP precursors were completely converted to HA without forming any other intermediate compounds such as  $\text{CaHPO}_4 \cdot 2\text{H}_2\text{O}$  (dicalcium phosphate dihydrate) and  $\text{Ca}_8(\text{HPO}_4)_2(\text{PO}_4)_4 \cdot 5\text{H}_2\text{O}$  (octacalcium phosphate). The shape of sharp diffraction peaks indicated that the HA bioceramics were fairly well crystallized (Figure 2C).

### Cell attachment assay

The morphology and distribution of hPDLSCs after 6 hours of culture on the bioceramics were observed by CLSM. Actin filaments were stained red by phalloidin. From Figure 3A, it can be observed that the hPDLSCs attached on the control HA demonstrated round and small configuration, while the cells attached on mnHA showed large and fibroblast-like

appearance (Figure 3B). Compared to the control HA sample, the cells spread on mnHA exhibited good adhesion, with more apparent cytoplasmic extension and more extended cytoplasmic processes. On the other hand, it can be observed that actin filaments of the cells adhering on mnHA were arranged regularly and parallel to the long axis of the cells, while the actin cytoskeleton formation on control HA was distributed irregularly.

Moreover, SEM imaging was further applied to illustrate the effect of surface topography on cell adhesion at 6 hours after cell seeding. As shown in Figure 4A and B, hPDLSCs adhered on mnHA grew and spread better than the cells cultured on control HA, which appeared as a small and round morphology.

### Cell proliferation

MTT assay was used to assess the proliferation of hPDLSCs after being cultured on HA and mnHA for 1, 4, and 7 days, respectively. The results showed that after being incubated for 1, 4, and 7 days, the number of cells cultured on mnHA was significantly higher than that of the cells cultured on control HA ( $P < 0.05$ ) (Figure 5). These results demonstrated that the mnHA topography could stimulate the proliferation of hPDLSCs.

### ALP activity assay

As shown in Figure 6A and B, ALP staining showed that the cells seeded on mnHA bioceramics stained more darkly and extensively than the control HA bioceramics at day 10. Besides, ALP activity of the cells seeded on mnHA was significantly higher than that of the cells cultured on the control HA at days 4 and 7 ( $P < 0.05$ ) (Figure 6C).

### Quantitative real-time PCR assay

Moreover, in order to identify the differentiating effects of the surface topography on HA bioceramics, osteogenic-/cementogenic-related genes were analyzed by real-time PCR. After being cultured for 1 day, the gene expression of *Runx2* was significantly increased on mnHA bioceramics than that on control HA bioceramics, and decreased as the time extended, while the expression of other osteogenic gene such as *ALP*, *CEMP*, and *CAP* was enhanced after 4 days culture. When culture time was extended to 7 days, the gene expressions of *Runx2*, *ALP*, *OCN*, *CAP*, and *CEMP* on mnHA bioceramics was dramatically higher than those on the control HA bioceramics ( $P < 0.05$ ) (Figure 7A–E). As shown in Figure 7F and G, the gene expression of *LRP5* and  *$\beta$ -catenin*, which were the specific markers of canonical Wnt

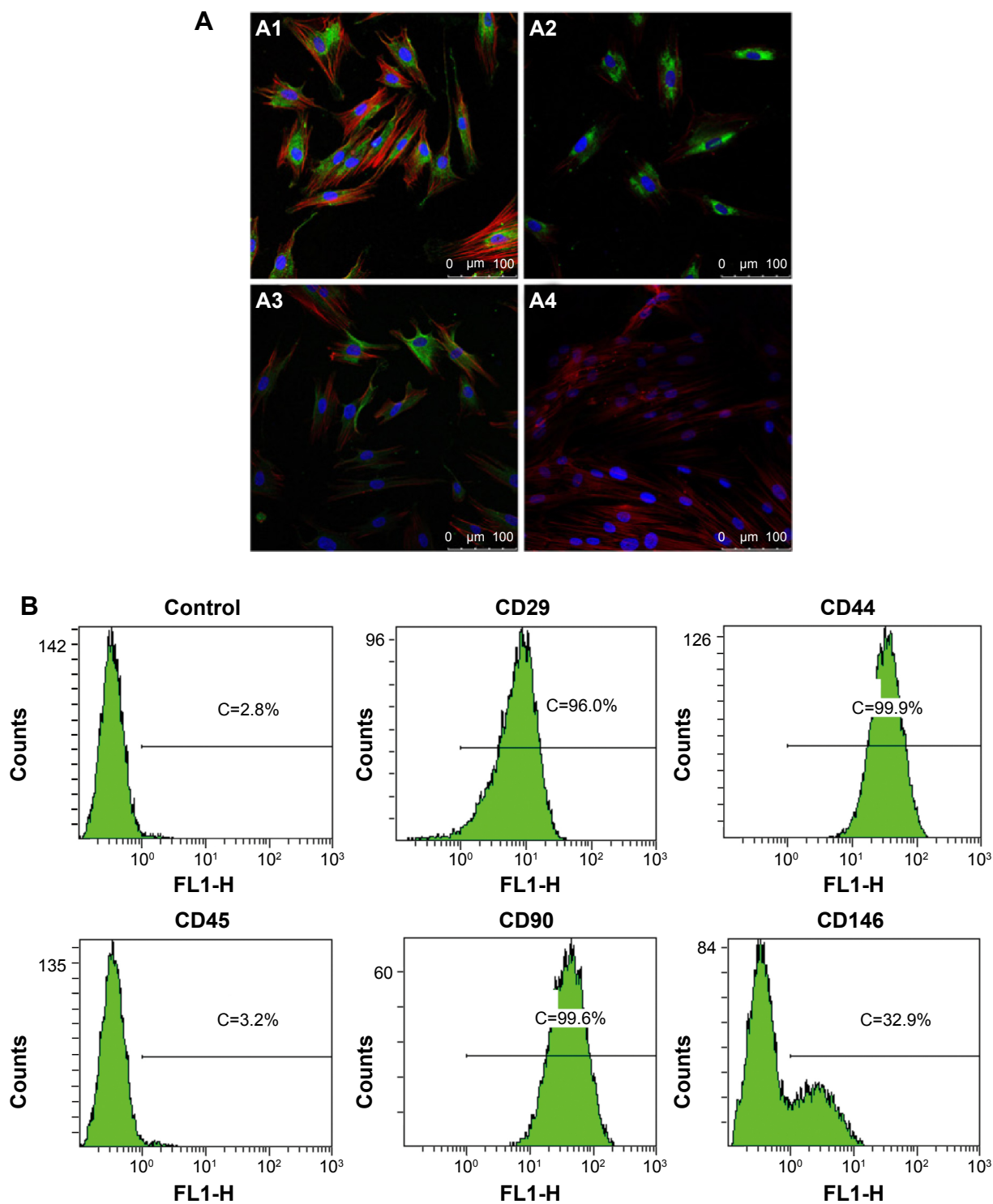


**Figure 1** Phenotypical characterization of hPDLSCs.

**Notes:** (A) Immunofluorescence staining of hPDLSCs for different markers. Cultured hPDLSCs exhibited positive staining for Vimentin (A1), S-100 (A2), STRO-1 (A3), and exhibited negative staining for CK (A4). The antibodies were stained green, the cytoskeletons were stained red, and the nuclei were stained blue. (B) The hPDLSCs were positive to CD29, CD44, CD90, and CD146 and negative to CD45. (A) Scale bar = 100 μm.

**Abbreviations:** hPDLSC, human periodontal ligament derived stem cell; CK, cytokeratin; C, counts.

signaling, was examined by real-time PCR after hPDLSCs were cultured on control HA and mnHA bioceramics for 1, 4, and 7 days, respectively. The result showed that the expression of LRP5 and  $\beta$ -catenin of mnHA group was

significantly higher than that of control HA group at day 1, and the levels of LRP5 and  $\beta$ -catenin of mnHA group were dramatically higher than that of the control HA group as the time extended. Especially, the gene levels of *LRP5* and

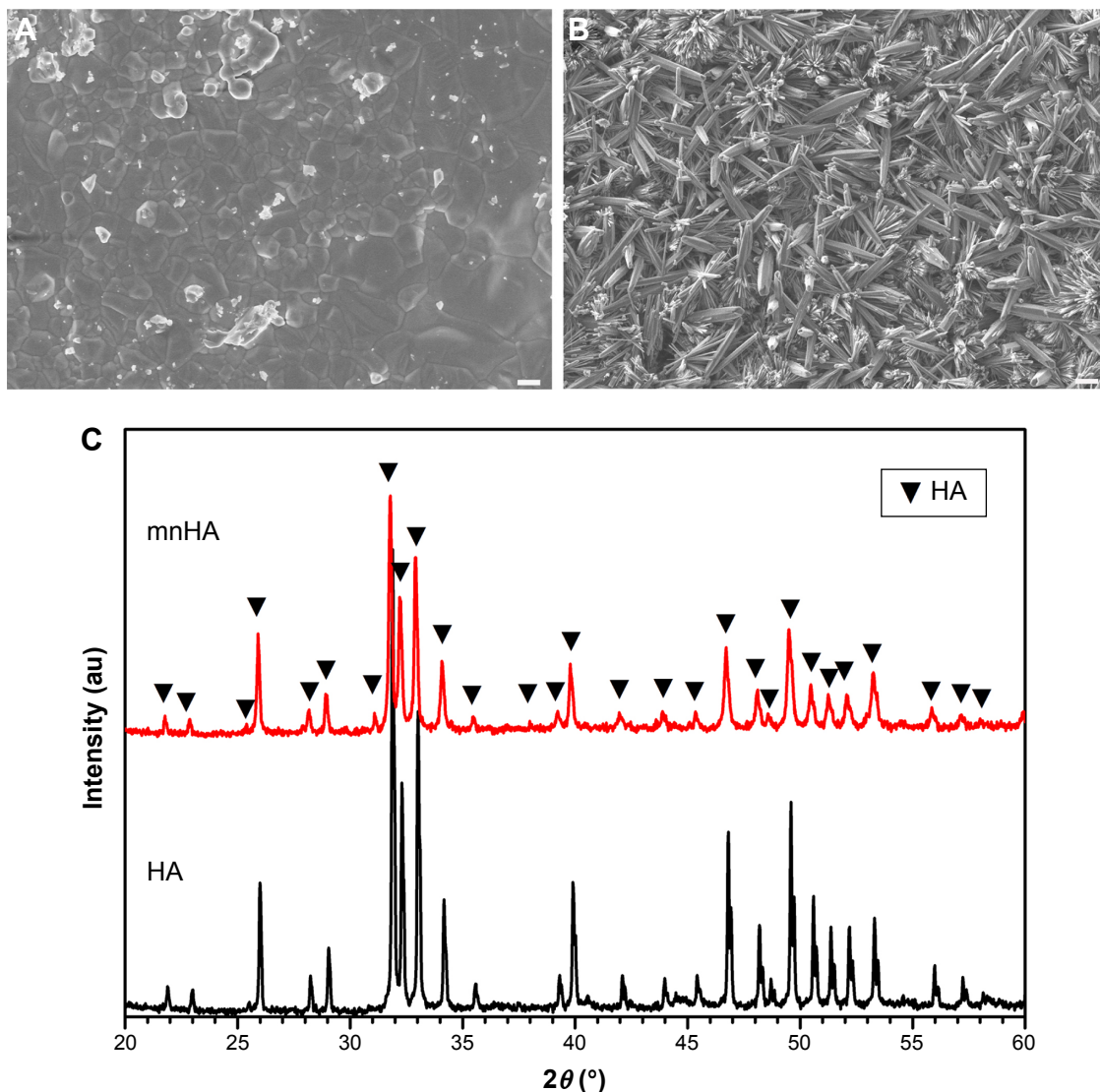


**Figure 2** Material characterization.

**Notes:** (A, B) SEM images of samples HA (A) and mnHA (B). (C) XRD patterns of samples HA and mnHA. (A) Scale bar = 1  $\mu\text{m}$ ; (B) Scale bar = 10  $\mu\text{m}$ .

**Abbreviations:** SEM, scanning electron microscopy; HA, hydroxyapatite; mnHA, micro-nano-hybrid surface; XRD, X-ray powder diffraction.

*$\beta$ -catenin* for hPDLSCs cultured on mnHA bioceramics were approximately 6.4–5.7-fold higher than those on the control HA group at day 7, respectively.

### Dkk1 treatment assay

Furthermore, to clarify the mechanism of whether the Wnt signaling pathway took part in the osteogenic/cementogenic differentiation of hPDLSCs cultured on mnHA bioceramics, exogenous Dkk1 (Wnt/ $\beta$ -catenin inhibitor) was applied to treat the hPDLSCs cultured on mnHA bioceramics. The results showed that exogenous Dkk1 obviously decreases the gene expression of *LRP5* and  *$\beta$ -catenin* after 7 days of culture (Figure 8A). Moreover, ALP activity (Figure 8B and C) and the gene expression of *Runx2*, *ALP*, *OCN*, *CAP*,

and *CEMP* were significantly attenuated by the application of Dkk1 at day 7 (Figure 8C).

### Discussion

Regeneration of the lost periodontium is a challenge in those both hard (alveolar bone, cementum) and soft (periodontal ligament) connective tissues, which need to be restored to their original architecture. PDLSCs possess multidifferentiation potential and exhibit an immunophenotype similar to BMSCs.<sup>7</sup> In this study, the characterization of hPDLSCs has been verified by analyzing their expression profile for various stem cell markers. Our results showed that hPDLSCs positively expressed MSC markers, including CD29, CD44, CD90, CD146, and STRO-1, but were

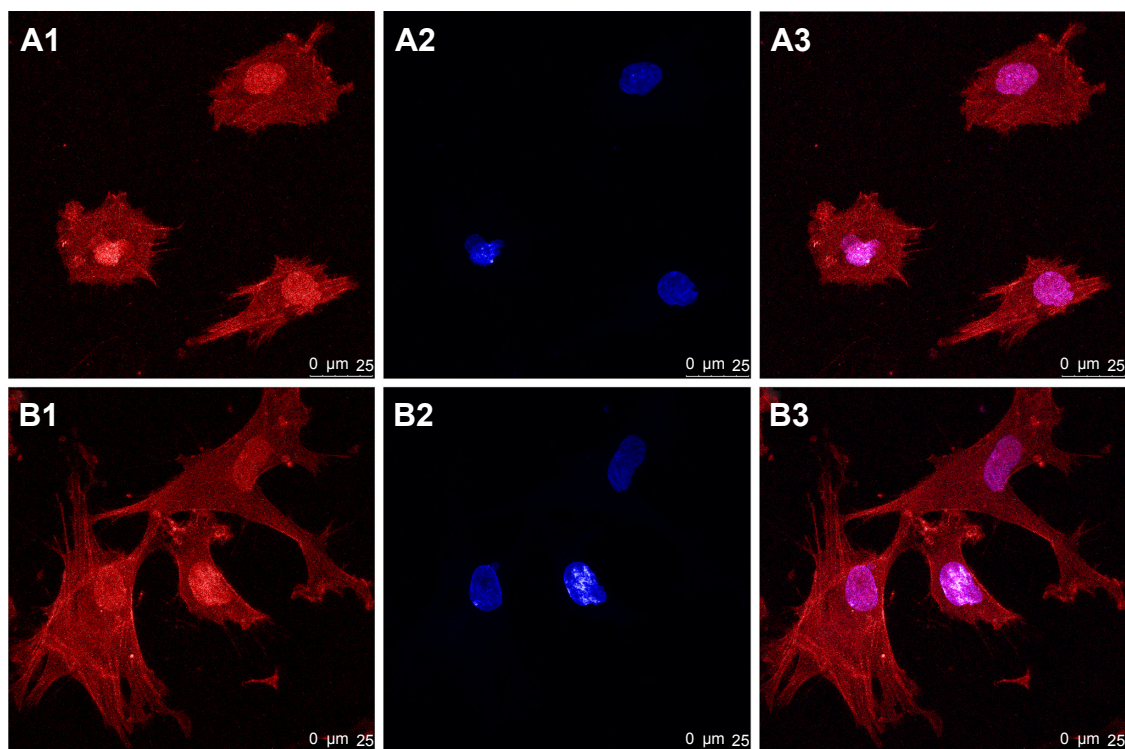


**Figure 3** CLSM images of hPDLSCs adhesion on HA (**A1–A3**) and mnHA (**B1–B3**) at 6 hours after seeding.

**Notes:** The actin filament was stained red by phalloidin (**A1, B1**) while the cell nuclei were stained blue by DAPI (**A2, B2**). (**A3, B3**) were the merge of (**A1, A2**) and (**B1, B2**) respectively. Scale bar =25  $\mu\text{m}$ .

**Abbreviations:** CLSM, confocal laser scanning microscope; hPDLSC, human periodontal ligament derived stem cell; HA, hydroxyapatite; mnHA, micro-nano-hybrid surface; DAPI, 4',6-diamidino-2-phenylindole dihydrochloride.

negative for hematopoietic lineage marker, including CD45, which is consistent with the previous report.<sup>33</sup> Moreover, we observed that 32.9% hPDLSCs expressed CD146, which can be taken to interpret that PDLSCs located in the perivascular wall of periodontal ligaments and express pericyte-specific markers CD146.<sup>34</sup> MSCs derived from some other tissues (bone marrow, skin, liver, lung) also express CD146.<sup>35</sup> More importantly, PDLSCs exhibited the abilities to form bone/cementum-like mineralized tissue and ligament structures similar to Sharpey's fibers with an associated

vasculature.<sup>8</sup> Traditional HA bioceramics, which possess good osteoconductivity and bioactivity, have been reported to combine with human periosteum-derived cells, acting as an osteogenic bone substitute for periodontal regenerative therapy.<sup>36</sup> However, traditional HA bioceramics lack the osteoinductive ability to induce osteogenic differentiation of stem cells and stimulate periodontal tissue regeneration, including bone and cementum.<sup>37</sup> Therefore, there is a requirement for modification of HA bioceramics to enhance their biological activity.

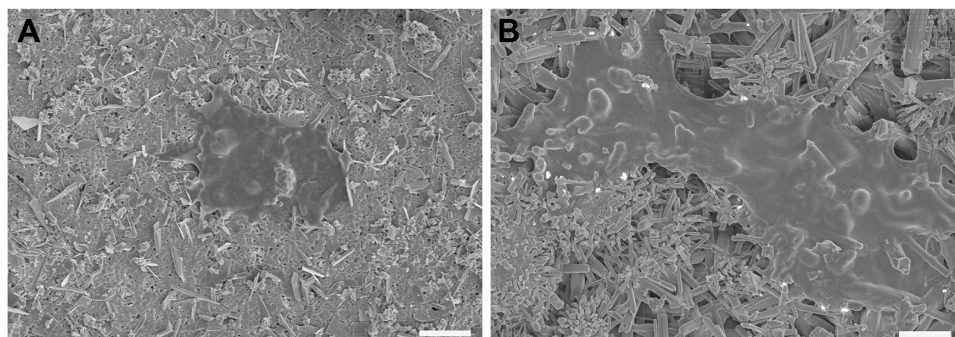


**Figure 4** SEM images of hPDLSCs on HA (**A**) and mnHA (**B**) after 6 hours of seeding.

**Note:** Scale bar =10  $\mu\text{m}$ .

**Abbreviations:** SEM, scanning electron microscopy; hPDLSC, human periodontal ligament derived stem cell; HA, hydroxyapatite; mnHA, micro-nano-hybrid surface.



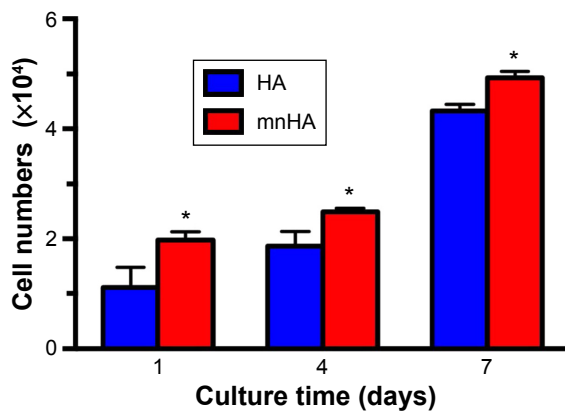


**Figure 5** MTT assay of hPDLSCs cultured on HA and mnHA for 1, 4, and 7 days. **Note:** \* $P < 0.05$ .

**Abbreviations:** hPDLSC, human periodontal ligament derived stem cell; HA, hydroxyapatite; mnHA, micro-nano-hybrid surface; MTT, 3-(4,5-dimethylthiazol-2-yl)-2,5-diphenyltetrazolium bromide.

Recent studies have indicated that the stem cell fate decision is strongly correlated to the biomaterial surface topography in tissue engineering and regenerative medicine.<sup>38</sup> It is reported that topographic features of material surface play an important role in adhesion, proliferation, differentiation,

and mineralization of stem cells.<sup>39</sup> It has been reported that the hybrid micro/nanoscale texture formed on the titanium surface could enhance the initial adhesion activity and osteogenic differentiation of BMSCs and MG63 cells in vitro<sup>40,41</sup> and promote bone formation in vivo.<sup>42</sup> In our previous studies, HA bioceramics with nanorod, nanosheet, and micro-nano-hybrid (the hybrid of nanorods and microrods) surfaces have been found to stimulate osteogenic differentiation of BMSCs and ASCs, while the mnHA possessed the best stimulation activity.<sup>18,20</sup> However, whether the micro/nano-structured HA bioceramics could promote PDLSCs differentiation into periodontal tissue was not known. In this study, we aimed at investigating the effects of HA bioceramics with mnHA on viability and osteogenic and cementogenic differentiation of hPDLSCs, which might estimate the possibility of micro/nano-structured HA bioceramics for periodontal tissue regeneration. The results of CLSM and SEM assays showed that hPDLSCs were found to attach better on mnHA bioceramics as compared with control HA bioceramics with flat and dense surface. Attributed to three-dimensional (3D) structure of mnHA surface,

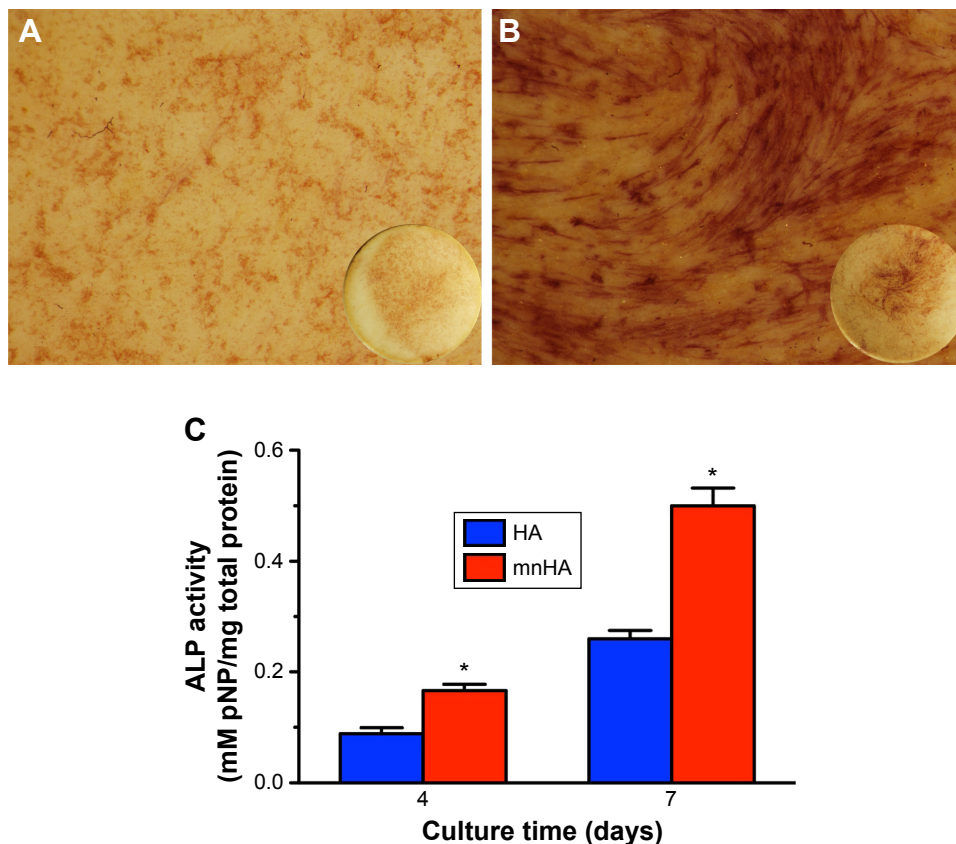


**Figure 6** ALP activity assay.

**Notes:** (A, B) ALP staining of hPDLSCs cultured on control HA (A) and mnHA (B) for 7 days. The circular insets show ALP staining of the whole disks; and the magnification of A and B is 10. (C) ALP activity quantitative analysis of hPDLSCs cultured on control HA and mnHA for 4 and 7 days. \* $P < 0.05$ .

**Abbreviations:** ALP, alkaline phosphatase; hPDLSC, human periodontal ligament derived stem cell; HA, hydroxyapatite; mnHA, micro-nano-hybrid surface; pNP, p-nitrophenol.

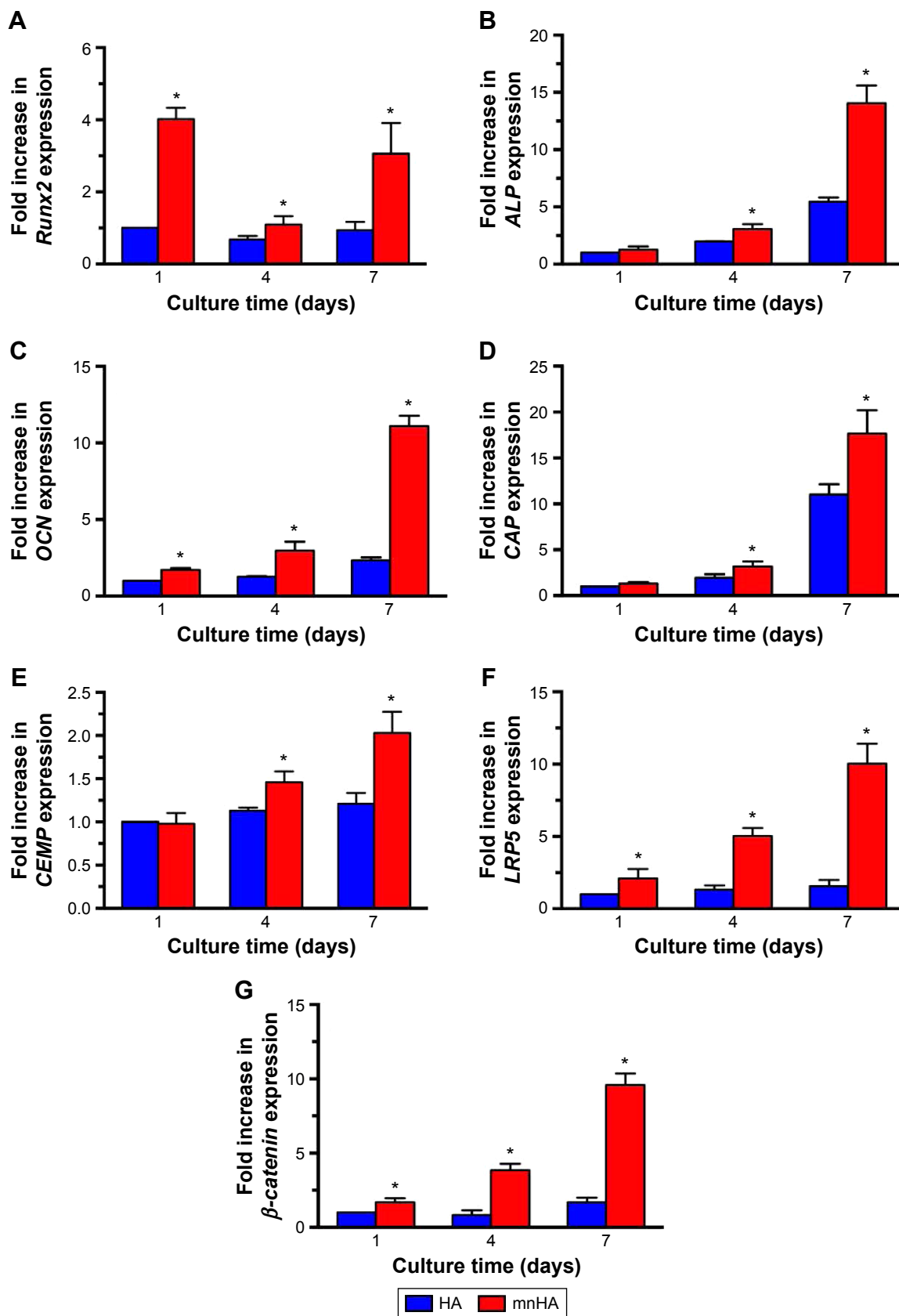


**Figure 7** The expression of osteogenic/cementogenic and Wnt signaling-related genes of hPDLS cells cultured on control HA and mnHA bioceramics for 1, 4, and 7 days.

**Notes:** (A) *Runx2*, (B) *ALP*, (C) *OCN*, (D) *CAP*, (E) *CEMP*, (F) *LRP5*, and (G)  $\beta$ -catenin. The expression level of mRNA was normalized to *GAPDH*. \* $P < 0.05$ .

**Abbreviations:** hPDLS, human periodontal ligament derived stem cell; HA, hydroxyapatite; mnHA, micro-nano-hybrid surface; *Runx2*, runt-related transcription factor 2; *ALP*, alkaline phosphatase; *OCN*, osteocalcin; *CAP*, cementum attachment protein; *CEMP*, cementum protein; *LRP5*, lipoprotein receptor-related protein 5; *GAPDH*, glyceraldehyde-3-phosphate dehydrogenase.

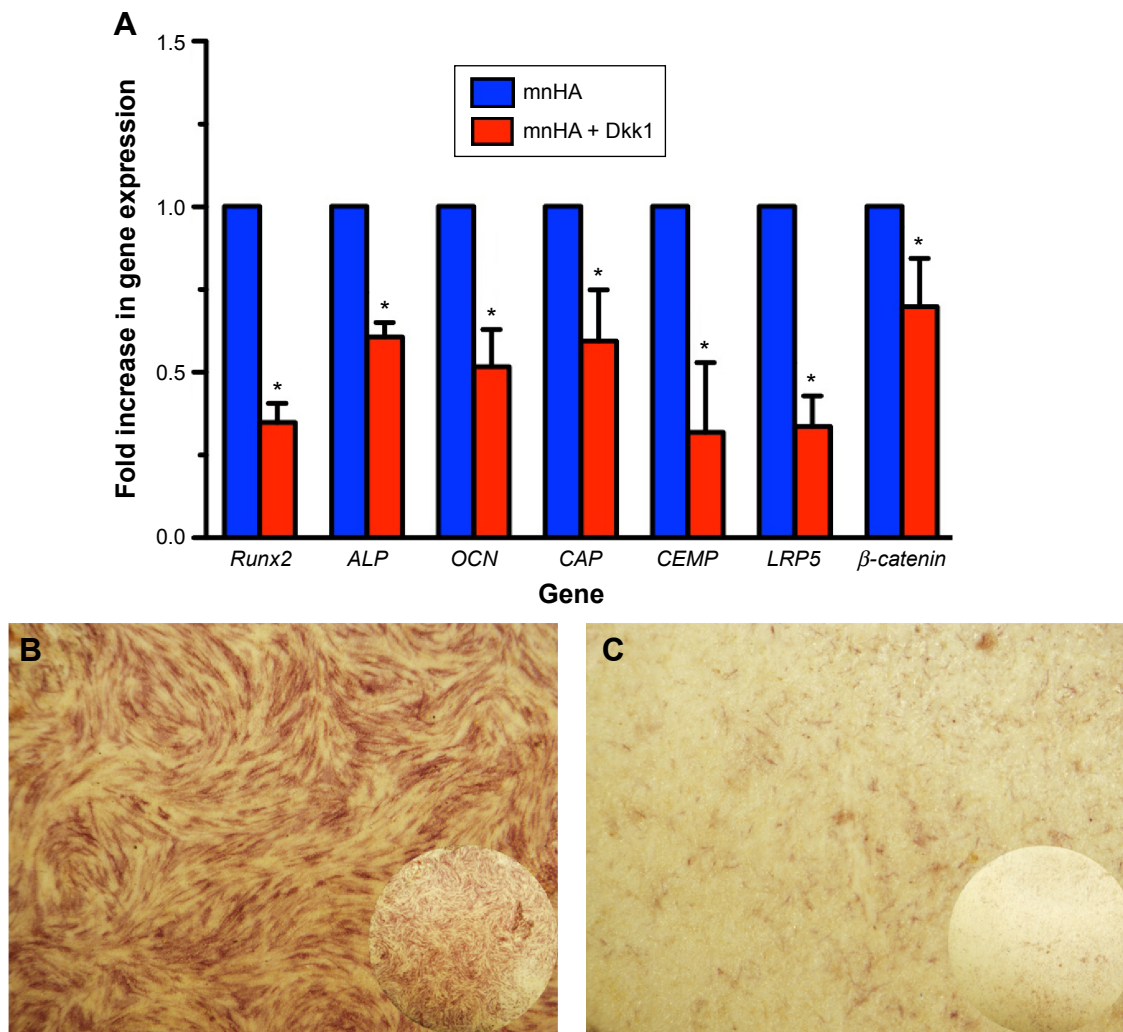


**Figure 8** The inhibition of Dkk1 on the osteogenic and cementogenic differentiation of hPDLSCs cultured on mnHA bioceramics.

**Notes:** (A) The expression of osteogenic/cementogenic and Wnt signaling-related genes for hPDLSCs cultured on mnHA ceramics or with Wnt signaling pathway inhibitor Dkk1 treatment at day 7. The expression level of mRNA was normalized to GAPDH. \* $P < 0.05$ . (B, C) ALP staining for hPDLSCs was performed on mnHA bioceramics (B) or with Wnt signaling pathway inhibitor Dkk1 treatment (C) at day 7. The circular insets show the whole disks; and the magnification of B and C is 10. **Abbreviations:** Dkk1, dickkopf1; hPDLSC, human periodontal ligament derived stem cell; mnHA, micro-nano-hybrid surface; *Runx2*, runt-related transcription factor 2; *ALP*, alkaline phosphatase; *OCN*, osteocalcin; *CAP*, cementum attachment protein; *CEMP*, cementum protein; *LRP5*, lipoprotein receptor-related protein 5; *GAPDH*, glyceraldehyde-3-phosphate dehydrogenase.

the contact area between cell and bioceramic surface was increased and the extension of the pseudopods of hPDLSCs into the 3D nanostructures resulted in much more extended shape, which is consistent with our previous studies.<sup>19</sup> A previous study has shown better cell attachment, and the spreading could enhance cellular functions including proliferation, migration, and extracellular matrix production.<sup>19</sup> In the present study, the result of MTT assay also showed that the micro-nano-hybrid topography could promote the proliferation of hPDLSCs.

ALP activity represents the early stage of osteoblast differentiation, which could regulate the degradation of inorganic pyrophosphate to provide sufficient local concentration of phosphate for mineralization.<sup>17,19</sup> After being cultured for 4 days, ALP activity in PDLSCs seeded on

HA bioceramics with mnHA was significantly higher than that in the control sample. Moreover, ALP activity in the two groups peaked after 7 days, and a more significant difference appeared between the two groups. Real-time PCR analysis of osteogenic and cementogenic gene expression further demonstrated that the surface microenvironment of bioceramics could regulate osteogenic differentiation of the cells. The gene expression of *Runx2*, *ALP*, and *OCN* was slightly upregulated on HA bioceramics with mnHA at day 4 and significantly enhanced at day 7, while little change was found in the control group. Considering the differences between the two groups, it could be suggested that surface topography may be the preliminary factor enhancing the osteogenic differentiation of hPDLSCs. These results are similar to our previous studies regarding to BMSCs and

ASCs.<sup>18,20</sup> In addition to upregulation of osteogenic-related genes, we also found that the cementum-specific markers, including CAP and CEMP, were enhanced in this study. The CAP has been shown to play an essential role in cell recruitment and differentiation during cementum formation, and periodontal cells that strongly bind to CAP are able to form cemented-like mineralized tissue in culture.<sup>43</sup> CEMP is specifically expressed in mature cementum matrix of adult periodontium and cementoblasts,<sup>40</sup> and it plays a key role in the local metabolism and as a differentiation regulator in PDL cells.<sup>44</sup> The high expression levels of CAP and CEMP for hPDLSCs seeded on HA bioceramics with mnHA suggest that mnHA modification of HA bioceramics may be a promising strategy for enhancing cementogenic differentiation of hPDLSCs and promoting the regeneration of the periodontal tissue.

Our previous study demonstrated that HA bioceramics with mnHA could enhance osteogenic differentiation of BMSCs via activation of ERK and p38 signaling pathways,<sup>20</sup> and Akt signaling pathway plays an important role in the effect of mnHAs on ASCs.<sup>18</sup> Whether there are any other signaling pathways involved in the effect of mnHA topography is unknown. The canonical Wnt signaling pathway is known to be crucial for skeletal development and homeostasis<sup>45,46</sup> and also plays an important role in bone formation and regeneration.<sup>47,48</sup> When Wnt pathway is not activated, LRP and FZD are bound to Wnt and the cytosolic protein  $\beta$ -catenin is phosphorylated by the heterotetrameric “destruction complex”, which consists of the Axin, APC, CK1, and GSK3. In response to activation of canonical Wnt signaling pathway, binding of DSH to the cytoplasmic tail of FZD results in recruitment of Axin from the destruction complex and FRAT1, followed by phosphorylation of LRP. As a consequence, nonphosphorylated  $\beta$ -catenin from the destruction complex and FRAT1 translocate into the nucleus to react with TCF/LEF transcription factors and regulate downstream genes, including those involved in bone formation, such as *Runx2*, *Col-1*, and *OPN* is induced.<sup>49</sup> It has been reported that Wnt/ $\beta$ -catenin signaling pathway mediates the biological effects of the microstructured titanium surface,<sup>50,51</sup> while the accumulated data suggests that activation of Wnt signaling is required for regeneration of periodontal tissues such as cementum, periodontal ligament, and alveolar bone.<sup>25,52</sup> Also, it has been reported that temporospatial regulation of Wnt/ $\beta$ -catenin signaling plays an important role in cell differentiation and matrix formation during root and cementum formation.<sup>53</sup> A recent study also showed that the activation of the canonical Wnt signaling pathway

can induce in vivo cementum regeneration and in vitro cementogenic differentiation of hPDLSCs.<sup>24</sup> In this study, the result of real-time PCR assay showed that the expression of canonical Wnt/ $\beta$ -catenin signaling-related genes such as *LRP5* and  *$\beta$ -catenin* of hPDLSCs on mnHA was significantly higher than that in the control group after being cultured for 1, 4, and 7 days.  $\beta$ -Catenin is the key factor of the canonical Wnt signaling pathway and plays an important role in cell proliferation and differentiation processes.<sup>54</sup> The *LRP5* gene is known as a coreceptor of Wnt and plays an important role in the development and maintenance of several tissues. *LRP5* could help regulate bone mineral density, and loss of this gene results in reduced skeletal strength, while gain of function results in higher bone mass.<sup>55,56</sup> The higher expression level of LRP5 and  $\beta$ -catenin for hPDLSCs cultured on HA bioceramics with mnHA indicates that the Wnt/ $\beta$ -catenin pathway is activated and consequently regulates osteogenic and cementogenic differentiation of hPDLSCs. To further verify the role of the Wnt signaling pathway in osteogenic and cementogenic differentiation of hPDLSCs by mnHA, Wnt antagonist Dkk1 was applied to block the canonical Wnt signaling pathway. Dkk1, a secreted inhibitor of the Wnt/ $\beta$ -catenin pathway, is a negative regulator of bone formation.<sup>57</sup> A previous study<sup>25</sup> found that blockage of canonical Wnt signaling by treating PDLCs with Dkk1 could inhibit Wnt-stimulated mRNA expression of *Runx2*, *Msx2*, and *Osterix2*, and the Wnt-enhanced ALP activity and matrix mineralization could be reduced by Dkk1 treatment.<sup>25</sup> The results showed that Dkk1 not only inhibited the expression of Wnt/ $\beta$ -catenin signaling-related genes (*LRP5* and  *$\beta$ -catenin*), but also reduced the ALP activity and the expression of osteogenic genes (*Runx2*, *ALP*, *OCN*) and cementogenic genes (*CAP* and *CEMP*), which are consistent with the previous reports. These results further confirmed that canonical Wnt/ $\beta$ -catenin signaling pathway was involved in the osteogenic/cementogenic differentiation of hPDLSC on mnHA group. Our data suggests that the canonical Wnt signaling plays an important role in the stimulatory effect of mnHA on hPDLSCs. However, the presence and function of Wnt-osteogenic/cementogenic pathway axis should be systematically evaluated in our future study. The future studies will be focused on the study of the effect of 3D macroporous HA scaffolds with micro-nano-hybrid structured surface on periodontal tissue repair in vivo.

## Conclusion

Present study revealed that HA bioceramics with mnHA significantly enhanced the cell attachment, spreading,

proliferation, and ALP activity of hPDLSCs. Moreover, the mnHA could not only enhance osteogenic but also cementogenic differentiation of hPDLSCs. Importantly, Wnt/ $\beta$ -catenin signaling pathway was involved in this process. It is suggested that HA bioceramics with mnHA may be promising grafting materials for periodontal tissue repair. However, further *in vivo* studies are required to confirm the periodontal regenerative effects.

## Acknowledgments

This study was supported by the National Natural Science Foundation of China (81371178 and 81171458), the Key Basic Research Foundation of the Shanghai Committee of Science and Technology, People's Republic of China (12JC1405700, 13NM1402102, and 15441905300), the Foundation of School of Medicine, Shanghai Jiao Tong University (12XJ10017), and the Biomedical Engineering Crossover Fund of Shanghai Jiao Tong University (YG2012MS40).

## Disclosure

The authors report no conflicts of interest in this work.

## References

- Nimigean VR, Nimigean V, Bencze MA, Dimcevic-Poesina N, Cergan R, Moraru S. Alveolar bone dehiscences and fenestrations: an anatomical study and review. *Rom J Morphol Embryol*. 2009;50(3):391–397.
- Rupprecht RD, Horning GM, Nicoll BK, Cohen ME. Prevalence of dehiscences and fenestrations in modern American skulls. *J Periodontol*. 2001;72(6):722–729.
- Nyman S, Gottlow J, Karring T, Lindhe J. The regenerative potential of the periodontal ligament. An experimental study in the monkey. *J Clin Periodontol*. 1982;9(3):257–265.
- Sanz AR, Carrion FS, Chaparro AP. Mesenchymal stem cells from the oral cavity and their potential value in tissue engineering. *Periodontol 2000*. 2015;67(1):251–267.
- Torii D, Konishi K, Watanabe N, Goto S, Tsutsui T. Cementogenic potential of multipotential mesenchymal stem cells purified from the human periodontal ligament. *Odontology*. 2015;103(1):27–35.
- Torii D, Tsutsui TW, Watanabe N, Konishi K. Bone morphogenetic protein 7 induces cementogenic differentiation of human periodontal ligament-derived mesenchymal stem cells. *Odontology*. Epub December 3, 2014.
- Seo BM, Miura M, Gronthos S, et al. Investigation of multipotent postnatal stem cells from human periodontal ligament. *Lancet*. 2004;364(9429):149–155.
- Menicanin D, Mrozik KM, Wada N, et al. Periodontal-ligament-derived stem cells exhibit the capacity for long-term survival, self-renewal, and regeneration of multiple tissue types *in vivo*. *Stem Cells Dev*. 2014; 23(9):1001–1011.
- Han J, Menicanin D, Gronthos S, Bartold PM. Stem cells, tissue engineering and periodontal regeneration. *Aust Dent J*. 2014;59(Suppl 1): 117–130.
- Adachi K, Amemiya T, Nakamura T, et al. Human periodontal ligament cell sheets cultured on amniotic membrane substrate. *Oral Dis*. 2014;20(6):582–590.
- Gronthos S, Mrozik K, Shi S, Bartold PM. Ovine periodontal ligament stem cells: isolation, characterization, and differentiation potential. *Calcif Tissue Int*. 2006;79(5):310–317.
- Liu Y, Zheng Y, Ding G, et al. Periodontal ligament stem cell-mediated treatment for periodontitis in miniature swine. *Stem Cells*. 2008;26(4):1065–1073.
- Dunaev MV, Kitaev VA, Matavkina MV, Druzhinin AE, Bubnov AS. Comparative analysis and clinical experience with osteoplastic materials based on non-demineralized bone collagen and artificial hydroxylapatite at the close of bone defects in ambulatory surgical dentistry. *Vestn Ross Akad Med Nauk*. 2014;(7–8):112–120.
- Zhou Y, Wu C, Xiao Y. The stimulation of proliferation and differentiation of periodontal ligament cells by the ionic products from Ca7Si2P2O16 bioceramics. *Acta Biomater*. 2012;8(6):2307–2316.
- Ercan B, Webster TJ. Greater osteoblast proliferation on anodized nanotubular titanium upon electrical stimulation. *Int J Nanomedicine*. 2008;3(4):477–485.
- Meirelles L, Arvidsson A, Andersson M, Kjellin P, Albrektsson T, Wennerberg A. Nano hydroxyapatite structures influence early bone formation. *J Biomed Mater Res A*. 2008;87(2):299–307.
- Lovmand J, Justesen J, Foss M, et al. The use of combinatorial topographical libraries for the screening of enhanced osteogenic expression and mineralization. *Biomaterials*. 2009;30(11):2015–2022.
- Xia L, Lin K, Jiang X, et al. Effect of nano-structured bioceramic surface on osteogenic differentiation of adipose derived stem cells. *Biomaterials*. 2014;35(30):8514–8527.
- Lin K, Xia L, Gan J, et al. Tailoring the nanostructured surfaces of hydroxyapatite bioceramics to promote protein adsorption, osteoblast growth, and osteogenic differentiation. *ACS Appl Mater Interfaces*. 2013;5(16):8008–8017.
- Xia L, Lin K, Jiang X, Xu Y, Zhang M, Chang J. Enhanced osteogenesis through nano-structured surface design of macroporous hydroxyapatite bioceramic scaffolds via activation of ERK and p38 MAPK signaling pathways. *J Mater Chem B*. 2013;1(40):5403–5416.
- Piters E, Boudin E, Van Hul W. Wnt signaling: a win for bone. *Arch Biochem Biophys*. 2008;473(2):112–116.
- Maeda K, Takahashi N, Kobayashi Y. Roles of Wnt signals in bone resorption during physiological and pathological states. *J Mol Med (Berl)*. 2013;91(1):15–23.
- Bodine PV, Komm BS. Wnt signaling and osteoblastogenesis. *Rev Endocr Metab Disord*. 2006;7(1–2):33–39.
- Han P, Ivanovski S, Crawford R, Xiao Y. Activation of the canonical Wnt signaling pathway induces cementum regeneration. *J Bone Miner Res*. Epub January 1, 2015.
- Heo JS, Lee SY, Lee JC. Wnt/ $\beta$ -catenin signaling enhances osteoblastogenic differentiation from human periodontal ligament fibroblasts. *Mol Cells*. 2010;30(5):449–454.
- Wang W, Zhao L, Ma Q, Wang Q, Chu PK, Zhang Y. The role of the Wnt/ $\beta$ -catenin pathway in the effect of implant topography on MG63 differentiation. *Biomaterials*. 2012;33(32):7993–8002.
- Han P, Wu C, Chang J, Xiao Y. The cementogenic differentiation of periodontal ligament cells via the activation of Wnt/ $\beta$ -catenin signalling pathway by Li<sup>+</sup> ions released from bioactive scaffolds. *Biomaterials*. 2012;33(27):6370–6379.
- Galli C, Piemontese M, Lumetti S, Manfredi E, Macaluso GM, Passeri G. GSK3 $\beta$ -inhibitor lithium chloride enhances activation of Wnt canonical signaling and osteoblast differentiation on hydrophilic titanium surfaces. *Clin Oral Implants Res*. 2013;24(8):921–927.
- Xia L, Feng B, Wang P, et al. *In vitro* and *in vivo* studies of surface-structured implants for bone formation. *Int J Nanomedicine*. 2012;7: 4873–4881.
- Yu J, He H, Tang C, et al. Differentiation potential of STRO-1+ dental pulp stem cells changes during cell passaging. *BMC Cell Biol*. 2010; 11:32.
- Shi S, Gronthos S. Perivascular niche of postnatal mesenchymal stem cells in human bone marrow and dental pulp. *J Bone Miner Res*. 2003;18(4): 696–704.
- Zhou Y, Wu Y, Jiang X, et al. The effect of quercetin on the osteogenic differentiation and angiogenic factor expression of bone marrow-derived mesenchymal stem cells. *PLoS One*. 2015;10(6):e0129605.

33. Wada N, Menicanin D, Shi S, Bartold PM, Gronthos S. Immunomodulatory properties of human periodontal ligament stem cells. *J Cell Physiol.* 2009;219(3):667–676.
34. Iwasaki K, Komaki M, Yokoyama N, et al. Periodontal ligament stem cells possess the characteristics of pericytes. *J Periodontol.* 2013;84(10):1425–1433.
35. Covas DT, Panepucci RA, Fontes AM, et al. Multipotent mesenchymal stromal cells obtained from diverse human tissues share functional properties and gene-expression profile with CD146+ perivascular cells and fibroblasts. *Exp Hematol.* 2008;36(5):642–654.
36. Kawase T, Okuda K, Kogami H, et al. Human periosteum-derived cells combined with superporous hydroxyapatite blocks used as an osteogenic bone substitute for periodontal regenerative therapy: an animal implantation study using nude mice. *J Periodontol.* 2010;81(3):420–427.
37. Yuan H, Fernandes H, Habibovic P, et al. Osteoinductive ceramics as a synthetic alternative to autologous bone grafting. *Proc Natl Acad Sci U S A.* 2010;107(31):13614–13619.
38. Kolind K, Kraft D, Boggild T, et al. Control of proliferation and osteogenic differentiation of human dental-pulp-derived stem cells by distinct surface structures. *Acta Biomater.* 2014;10(2):641–650.
39. Zhang J, Luo X, Barbieri D, et al. The size of surface microstructures as an osteogenic factor in calcium phosphate ceramics. *Acta Biomater.* 2014;10(7):3254–3263.
40. Wang W, Liu Q, Zhang Y, Zhao L. Involvement of ILK/ERK1/2 and ILK/p38 pathways in mediating the enhanced osteoblast differentiation by micro/nanotopography. *Acta Biomater.* 2014;10(8):3705–3715.
41. Zhang W, Li Z, Huang Q, et al. Effects of a hybrid micro/nanorod topography-modified titanium implant on adhesion and osteogenic differentiation in rat bone marrow mesenchymal stem cells. *Int J Nanomedicine.* 2013;8:257–265.
42. Branemark R, Emanuelsson L, Palmquist A, Thomsen P. Bone response to laser-induced micro- and nano-size titanium surface features. *Nanomedicine.* 2011;7(2):220–227.
43. Valdes De Hoyos A, Hoz-Rodriguez L, Arzate H, Narayanan AS. Isolation of protein-tyrosine phosphatase-like member-a variant from cementum. *J Dent Res.* 2012;91(2):203–209.
44. Hoz L, Romo E, Zeichner-David M, et al. Cementum protein 1 (CEMP1) induces differentiation by human periodontal ligament cells under three-dimensional culture conditions. *Cell Biol Int.* 2012;36(2):129–136.
45. Tamura M, Nemoto E, Sato MM, Nakashima A, Shimauchi H. Role of the Wnt signaling pathway in bone and tooth. *Front Biosci (Elite Ed).* 2010;2:1405–1413.
46. Xu H, Duan J, Ning D, et al. Role of Wnt signaling in fracture healing. *BMB Rep.* 2014;47(12):666–672.
47. Kim JB, Leucht P, Lam K, et al. Bone regeneration is regulated by wnt signaling. *J Bone Miner Res.* 2007;22(12):1913–1923.
48. Kobayashi Y. Roles of Wnt signaling in bone metabolism. *Clin Calcium.* 2012;22(11):1701–1706.
49. Baron R, Rawadi G, Roman-Roman S. Wnt signaling: a key regulator of bone mass. *Curr Top Dev Biol.* 2006;76:103–127.
50. Olivares-Navarrete R, Hyzy S, Wieland M, Boyan BD, Schwartz Z. The roles of Wnt signaling modulators Dickkopf-1 (Dkk1) and Dickkopf-2 (Dkk2) and cell maturation state in osteogenesis on microstructured titanium surfaces. *Biomaterials.* 2010;31(8):2015–2024.
51. Olivares-Navarrete R, Hyzy SL, Park JH, et al. Mediation of osteogenic differentiation of human mesenchymal stem cells on titanium surfaces by a Wnt-integrin feedback loop. *Biomaterials.* 2011;32(27):6399–6411.
52. Kim TH, Lee JY, Baek JA, et al. Constitutive stabilization of  $\beta$ -catenin in the dental mesenchyme leads to excessive dentin and cementum formation. *Biochem Biophys Res Commun.* 2011;412(4):549–555.
53. Bae CH, Lee JY, Kim TH, et al. Excessive Wnt/ $\beta$ -catenin signaling disturbs tooth-root formation. *J Periodontol Res.* 2013;48(4):405–410.
54. Yan Y, Tang D, Chen M, et al. Axin2 controls bone remodeling through the  $\beta$ -catenin-BMP signaling pathway in adult mice. *J Cell Sci.* 2009;122(Pt 19):3566–3578.
55. Thorfve A, Lindahl C, Xia W, et al. Hydroxyapatite coating affects the Wnt signaling pathway during peri-implant healing in vivo. *Acta Biomater.* 2014;10(3):1451–1462.
56. Lim WH, Liu B, Mah SJ, Yin X, Helms JA. Alveolar bone turnover and periodontal ligament width are controlled by Wnt. *J Periodontol.* 2015;86(2):319–326.
57. Menezes ME, Devine DJ, Shevde LA, Samant RS. Dickkopf1: a tumor suppressor or metastasis promoter? *Int J Cancer.* 2012;130(7):1477–1483.

## International Journal of Nanomedicine

### Publish your work in this journal

The International Journal of Nanomedicine is an international, peer-reviewed journal focusing on the application of nanotechnology in diagnostics, therapeutics, and drug delivery systems throughout the biomedical field. This journal is indexed on PubMed Central, MedLine, CAS, SciSearch®, Current Contents®/Clinical Medicine,

Submit your manuscript here: <http://www.dovepress.com/international-journal-of-nanomedicine-journal>

Dovepress

Journal Citation Reports/Science Edition, EMBASE, Scopus and the Elsevier Bibliographic databases. The manuscript management system is completely online and includes a very quick and fair peer-review system, which is all easy to use. Visit <http://www.dovepress.com/testimonials.php> to read real quotes from published authors.